IONIC CONDUCTIVITY

IN BRAGG

GLASSES

By

LYNETT MICHELLE ROCK

Bachelor of Science

Northeastern State University

Tahlequah, Oklahoma

1994

Submitted to the Faculty of the
Graduate college of the
Oklahoma State University
in partial fulfillment of
the requirements for
the Degree of
MASTER OF SCIENCE
July, 1996

IONIC CONDUCTIVITY

IN BRAGG

GLASSES

Thesis Approved:

Thesis Advisor

Dean of the Graduate College

ACKNOWLEDGMENTS

I would like to express my gratitude to my Major Advisor, Dr. George Dixon for giving me a chance. Without Dr. Dixon's guidance and patience, this thesis would not exist. I would also like to extend my thanks to my other committee members Dr. Joel Martin and Dr. Donna Bandy. Dr. Martin always offered a smile and words of encouragement when I passed by his door on my way to see Dr. Dixon.

I would like to extend my undying appreciation to my parents, Joyce and Calvin Rock. When I wanted to give up, Mom gave me no choice. They pushed me when my own strength failed and applauded when I succeeded. This thesis is more for them than for me. I also wish to express my sincere gratitude to my husband, Jason Crull. Jason listened to me complain about this day out and day in for months. He deserves more than my thanks, he deserves a vacation. I also want to thank my daughter Scarlet, she inspired me by saying nothing and giving me a chance to escape.

Last, but not Least, I want to thank my friends in the physics department. John, Mike, Brain, Von, Serge, and Anne; you people made me laugh at myself and then pick up and move on. I don't believe that I would have made it without you, thanks for your help and for just listening to me when I needed someone to abuse.

TABLE OF CONTENTS

LIST OF TABLES

LIST OF FIGURES

Chapter I

Introduction

Ion Transport

Although one usually thinks of transparent materials as electrical insulators, glass can support small electric currents through the motion of small ions. Such ionic currents, though small compared to the currents due to electronic conduction in metals and semiconductors, are typically much larger in glasses than they are in crystalline solids. In the latter case the ordered array of atoms in the crystal lattice prevents ionic migration except where there are defects in the crystal that disrupt its order. These defects include interstitial ions which are weakly bonded and can move through channels in the structure, and vacancies which provide sites that can be reached by ions in the lattice with only a small net expenditure of energy. It is inherent that all glasses contain a number of defects.[1]

Glasses are disordered materials, except on the scale of local chemical bonding. They are usually mixtures of covalently bonded substances, such as SiO_2, which form a continuous random network that is the backbone of the glass, and ionically bonded network modifiers, such as Na_2O or MgO, which attach themselves to the network and modify its structure. Glass technologist typically add network modifiers to lower the

melting point of glass, change its resistance to erosion by water, or give it color. Because of the disorder, many of the network modifiers are only weakly bonded and can move through the channels in the network much as interstitals move through crystals. Similarly, there often are many neighboring local minima in the potential energy that an ion would experience in the network; these can act to promote ionic motion in the same way that vacancies do in crystals. Figure 1.1 demonstrates how ions may move throughout the network of a glass.

Mobile ions create their own environments in the structure of the glass.[2] These distinctive environments are built throughout the glass when an ion occupies a specific position. When the ion moves forward the structure relaxes to the original position the glasses possessed before the ion interacted with it. The period needed for the structure to return to its original state is its relaxation time. Depending on the size of the ion and how long the position was occupied the relaxation time varies.

Mixed Alkali Effect

In this thesis, the mixed alkali effect will be discussed. This simply relates to more than one alkali present in a glass structure. There is a direct link between the ionic conductivity and the composition of the glass.[3] Therefore the addition of another alkali to the composition should effect the conductivity, implying that variations on the conductivity are related to the presence of certain chemical entities in the glass. Each alkali creates and maintains its own distinctive environment. The local environment of each alkali is largely unaffected by the addition of a second alkali.[2] Therefore each ion

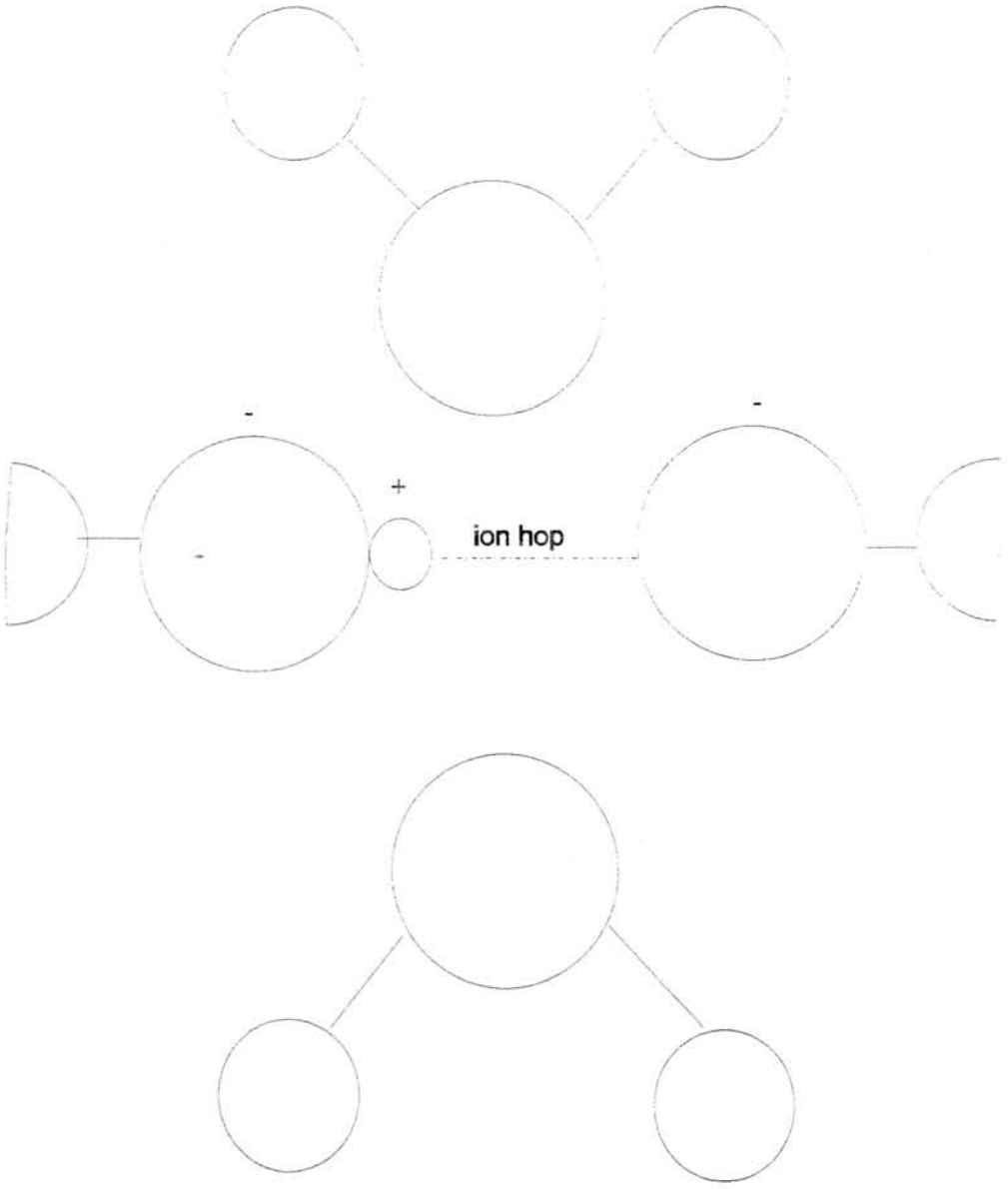

Figure 1.1: Systematic representation of ion hopping.

will stili posses its own receptor sites. It has been suggested that the sites occupied by alkalis in a mixed environment do not differ dramatically from the sites they would occupy in a single alkali glass.[4]

Suppose there are only two alkalis, A and B, present in the glass. Ion A will be inclined to jump to a vacancy ***A'*** that was previously occupied by an ion A. This implies that the ion A would decline to jump to a vacant site ***B'*** previously occupied by an ion B. This theory would imply that the structure of the glass had a "memory".[2] The ionic conductivity of glass with mixed alkali is notably smaller than the conductivity of glass that contain just one of the alkali present. This occurs due to the mismatch effect arising from different sizes and coordination requirements of different alkalis.[3] Common sense implies that if an ion is compelled to "worry" about being rejected by a vacant site that was previously occupied by a different type ion, that the ability to make the journey would be inhibited.

Since the conductivity is usually additive, the addition of a second or third alkali would imply an increase in conductivity. But alkali produce a unique effect, the conductivity of a mixed alkali glass is considerably lower than the corresponding single alkali glasses when subjected to similar temperatures.[5] This phenomenon moves mixed alkali glasses into their own category in the study of conductivity.

The mixed alkali effect could be expected due to earlier statements. Since every ion present in the glass modifies the structure to suit its own needs, this modification leads to slower relaxation times. Rapid exchange of sites is prohibited since time is needed to expand/contract the system to allow the different ions movement.

Activation Energy

The activation energy is the energy associated with one ion moving to another site. This energy combines the energy needed to breakout of the ions current position, along with the energy needed to move throughout the structure, and energy needed to occupy a new position. These activation energies must be overcome by cations moving into nearby empty sites.[6] Each type of ion that can travel throughout the structure possesses its own distinctive activation energy. The energy measured by the processes used in this thesis represent an affective activation energy in that it records an overall effect instead of activation energies of individual ions.

CHAPTER II

EXPERIMENTAL PROCEDURE

The Samples

In this thesis, four Bragg glass samples were examined. The samples used were Bragg 5, Bragg 11, Bragg 13, and Bragg 14. They are members of a series of glasses being studied for holographic grating formation. All of the samples had the same fundamental base, which when presented in a percentage of molar composition (mol%) is $70SiO_2$-$3Al_2O_3$-$12MgO$-$15Na_2O$. The first sample Bragg 5 was composed of this basic formulation. The second sample, Bragg 11, had a molar composition of $70SiO_2$-$3Al_2O_3$-$12MgO$-$7.5Na_2O$-$7.5Li_2O$. The third sample, Bragg 13, had a molar composition of $70SiO_2$-$3Al_2O_3$-$12MgO$-$7.5Na_2O$-$7.5K_2O$. The final sample, Bragg 14, had basically the same composition as Bragg 13 except it is also doped with Eu_2O_3. Therefore Bragg 14 molar composition was $68.3SiO_2$-$2.9Al_2O_3$-$11.7MgO$-$7.3Na_2O$-$7.3K_2O$-$2.5Eu_2O_3$. These samples and their properties are listed in Table I for easy reference. All of these samples were prepared by L. Pierre de Rochemont, C^2 Technologies, Hampton, New Hampshire.

TABLE I

SAMPLE COMPOSITION

Element	Bragg 5	Bragg 11	Bragg 13	Bragg 14
SiO_2	70	70	70	68.3
Al_2O_2	3	3	3	2.9
MgO	12	12	12	11.7
Na_2O	15	7.5	7.5	7.5
Li_2O	—	7.5	—	—
K_2O	—	—	7.5	7.3
Eu_2O_3	—	—	—	2.5

Each sample was cut so that the area was large in comparison to the thickness. After the samples were cut, they were polished to a surface finish of 1 micron with Metadi II diamond polishing compound, made by the Buehler company. The next step was to clean the samples. This was done with a combination of an ultra-sonic cleaner with distilled water and heating the samples in a furnace to dry them. Finally, a thin film of gold was placed onto the samples by an electrode-evaporator. The length, width, and area of the samples are located in Table II for easy reference.

Experimental Setup For Ionic Conductivity

This experiment was conducted under microcomputer control over a IEEE488 Bus interface. The samples were placed between two sheets of grafoil and then sandwiched between two bars connected to the power source and a picoammeter. Figure 2.1 shows a more detailed picture. The computer was connected, over the serial port RS232, to an Omega programmable temperature controller. This controller was connected to the furnace via a thermocouple and therefore controiled the power to the furnace.

The Omega controller regulated the temperature of the sample. It first heated the sample, from room temperature to a maximum temperature of 500°C. Then the sample was cooled back to room temperature. While this heating and cooling was occurring, the computer took integral readings of the current and temperature simultaneously. The computer was allowed to do so through the interface which was connected to a

TABLE II

SAMPLE DIMENSIONS

Sample	Length	Width	Thickness	Area
Bragg 5	0.745 cm	0.653 cm	0.157 cm	0.487 cm^2
Bragg 11	0.752 cm	0.475 cm	0.196 cm	0.357 cm^2
Bragg 13	1.01 cm	.0470 cm	0.119 cm	0.475 cm^2
Bragg14	0.774 cm	0.377 cm	0.111 cm	0.292 cm^2

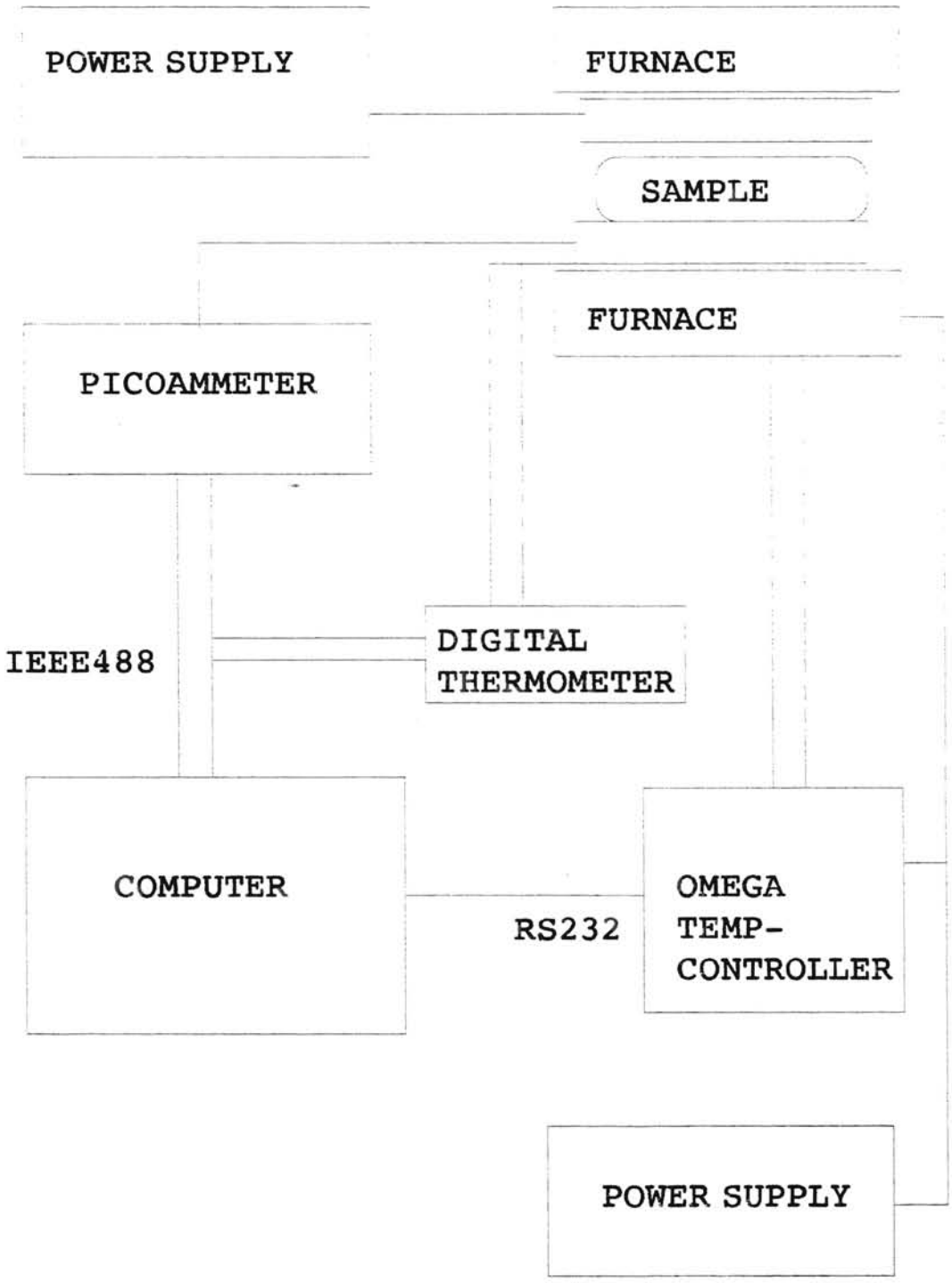

Figure 2.1: Detailed picture of experimental setup.

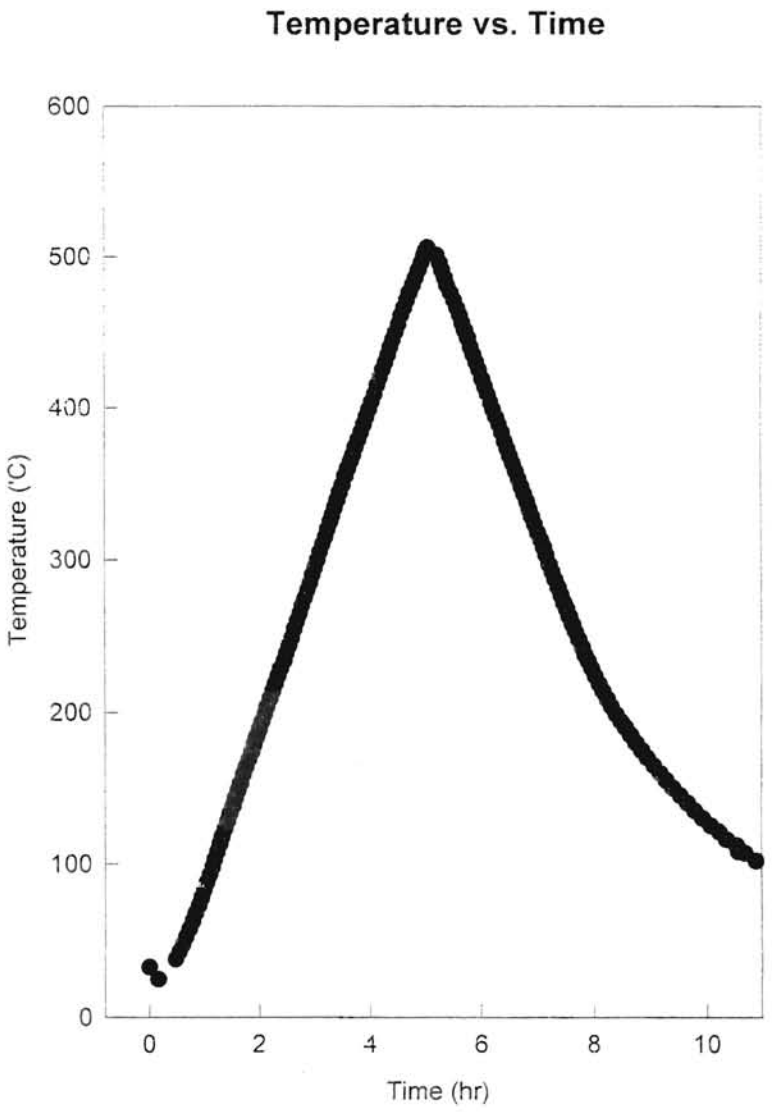

Figure 2.2: A typical Temperature vs. Time graph collected by the computer for one of the samples.

picoammeter and a digital thermometer. Figure 2.2 displays a typical temperature vs. time graph collected by the computer, while Figure 2.3 shows the corresponding current vs. time graph.

The sample was subjected to a constant voltage by a KEPCO power supply. All of the samples experienced a voltage of ± 25 volts. Using the current and temperature recorded, along with the constant voltage, the ionic conductivity can be calculated. The equation used to calculated the ionic conductivity is:

$$\sigma = (tI) / (VA).$$

Where t is the thickness in centimeters, I is the current measured at a specific temperature in amps, V is the applied voltage recorded in volts, and A is the area of the sample with units of cm^2. This gives units for the ionic conductivity of $1/\Omega cm$. Once the conductivity has been calculated a second equation needs to be considered. To find the activation energy for each sample, E, the following equation is needed.

$$\sigma = (Nq^2va^2 / k_bT)\exp(-E / k_bT)$$

Some clarification is now needed. In the above equation, N is the concentration of impurities within the sample. The charge of present ions is represented by q. The characteristic atomic vibrational frequency is referred to as v, while a is used to represent the lattice constant.[7] When examining this equation, it is noted that multiplying the equation by the temperature will make further evaluation simpler. The resulting equation is:

$$\sigma T = (Nq^2va^2 / k_b)\exp(-E / k_bT)$$

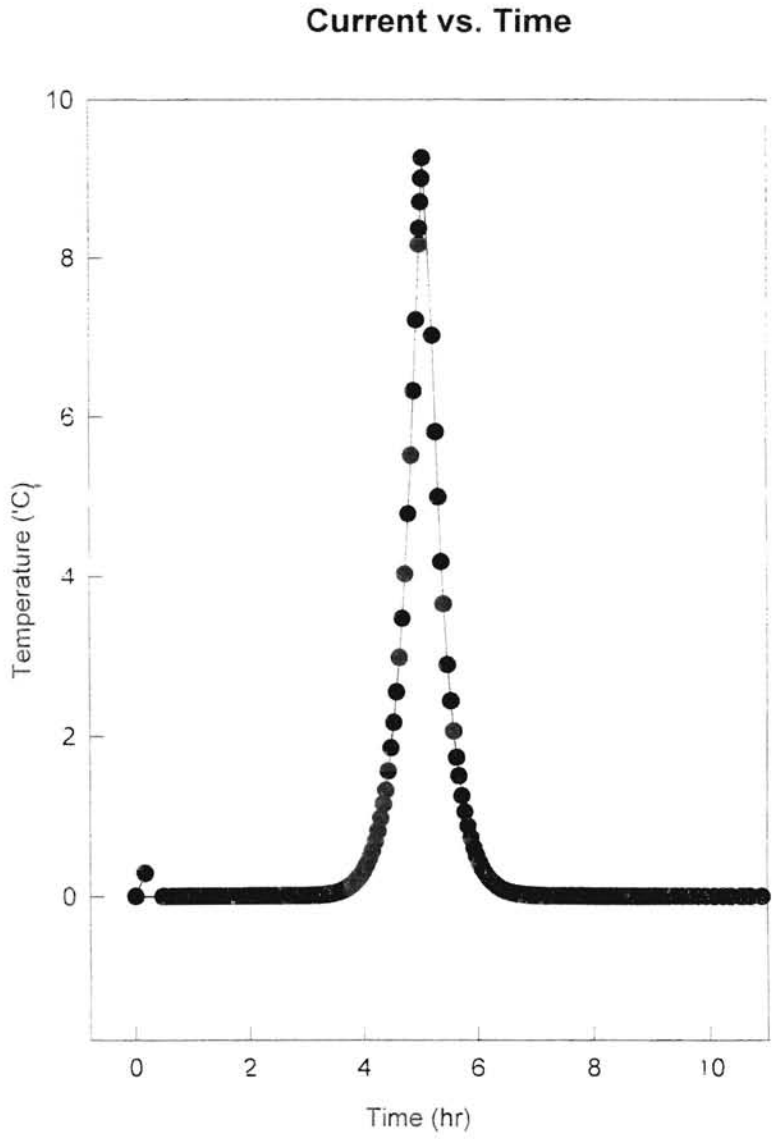

Figure 2.3: A typical Current vs: Time graph collected by the computer for one of the samples.

Now by taking the natural log of both sides of the equation, the following results is found.

$$\ln(\sigma T) = \ln(Nq^2va^2 / k_b) + (-E / k_bT)$$

Looking at the equation, it is noted that the first term on the right side of it is a constant, and so:

$$\ln(\sigma T) \cong -E / k_bT .$$

Using this final equation, and plotting ln(σT) vs. 1000/T the activation energy can be calculated from the slope. This will be discussed again in Chapter 3.

Chapter III

Results and Discussion

Electrical conduction in glasses is due almost exclusively to the motion of small cations, such as alkalis or alkaline earths, through channels in the glass matrix. The ionic conductivity for a single species of ion can be expressed as

$$\sigma = Nze\mu$$

where N is the number of free ions of a given type, z is its valance, e is the elementary charge, and μ is the mobility of the free ions. Here the free ions are those that have been thermally dissociated from their bonding anions, and represent in general only a fraction of the total ionic population of the glass. If there are multiple free ionic species the total conductivity is the sum of their individual conductivities

$$\sigma = \Sigma N_j z_j e \mu_j$$

as is the case for electron and hole conductivities in semiconductors.

As the thermal dissociation referred to above implies, it is of interest to measure the temperature dependence of the ionic conductivity of the glass. This allows an effective activation energy E_a to be extracted. This activation energy will consist of a largely electrostatic contribution E_B from the thermal dissociation of the anion and cation and also a contribution from the strain energy E_S associated with the opening of "doors"

in the network to allow the motion of the ion through the channels in the network [8]. This was demonstrated earlier in Chapter 1 with Figure 1.1. It is not possible to separate these two contributions to the activation energy in the ionic conductivity alone. The effective activation energy is $E_a=E_B+E_S$. However, it is possible to estimate E_a in the point ion approximation for a given alkali-containing cluster. Since E_S must be positive this may allow some sources for the free ions to be eliminated as too tightly bound to agree with the experiment. E_a is derived experimentally from

$$\sigma = AT^{-1}\exp(-E_a / k_b T)$$

In addition to the activation energy or energies, the magnitude of the conductivity as it is affected by the possible types of carriers present in the glass is of interest. It is known that in some glass compositions, the simple additivity described above does not hold, at least if one attempts to use conductivities derived from similar glasses with only a single type of mobile cation. This "mixed alkali effect" implies that the different chemical species interfere with each others' activation and/or mobility. We wish to know whether similar effects occur in the present glasses, as these will affect their suitability as substrates for laser-induced grating formation.

As we shall see below, the ionic conductivity measured by out technique is dependent of the electro-thermal history of the sample. Heating the sample to approximately 700 K under a 25 V field was sufficient to deplete the population of free carriers. This may be related to the observation that once a laser-induced grating has been written and erased, it is more difficult to rewrite a new grating in these glasses. The conductivity was observed to recover, and exhibit similar activation energies, when the potential difference across the sample was reversed.

When calculating the ionic conductivity, the initial and maximum value were noted for every run of all four samples. Figure 3.1 illustrates a typical graph of Conductivity vs. Temperature. The temperature dependence of the conductivity is usually Arrhenius.[9] Some exceptions always exist, but this thesis will assume all the samples fall into this category. It demonstrates how conductivity is dependent upon the temperature the sample is exposed to at a given time. A difference was distinguished between runs experiencing reversed polarity. Reversed polarity only implies that a negative voltage was applied to each sample throughout the data collection process. The initial magnitude for each sample was surprising similar. The magnitude of the largest value changes according the composition. Figure 3.2 through Figure 3.5 are typical graphs of ln(conductivity) vs. 1000/Temperature. From these graphs it is simple to estimate the maximum and initial conductivity of each sample. For further simplification, Table III contains the initial and maximum conductivity for each sample and run.

Using Bragg 5 as the control group, the following results were noted. When the smallest of the ions, Lithium, was added the ionic conductivity increased. While with the presence of a larger ion, potassium, the ionic conductivity decreased. An explanation is offered regarding the conductivity collected in this thesis. When an ion is added to the network it modifies a place for itself. When it becomes time for the ions to move, a new space needs to be prepared. When a smaller ion moves it could be suggested that modification of the network would be simpler. With less modification of the network, it

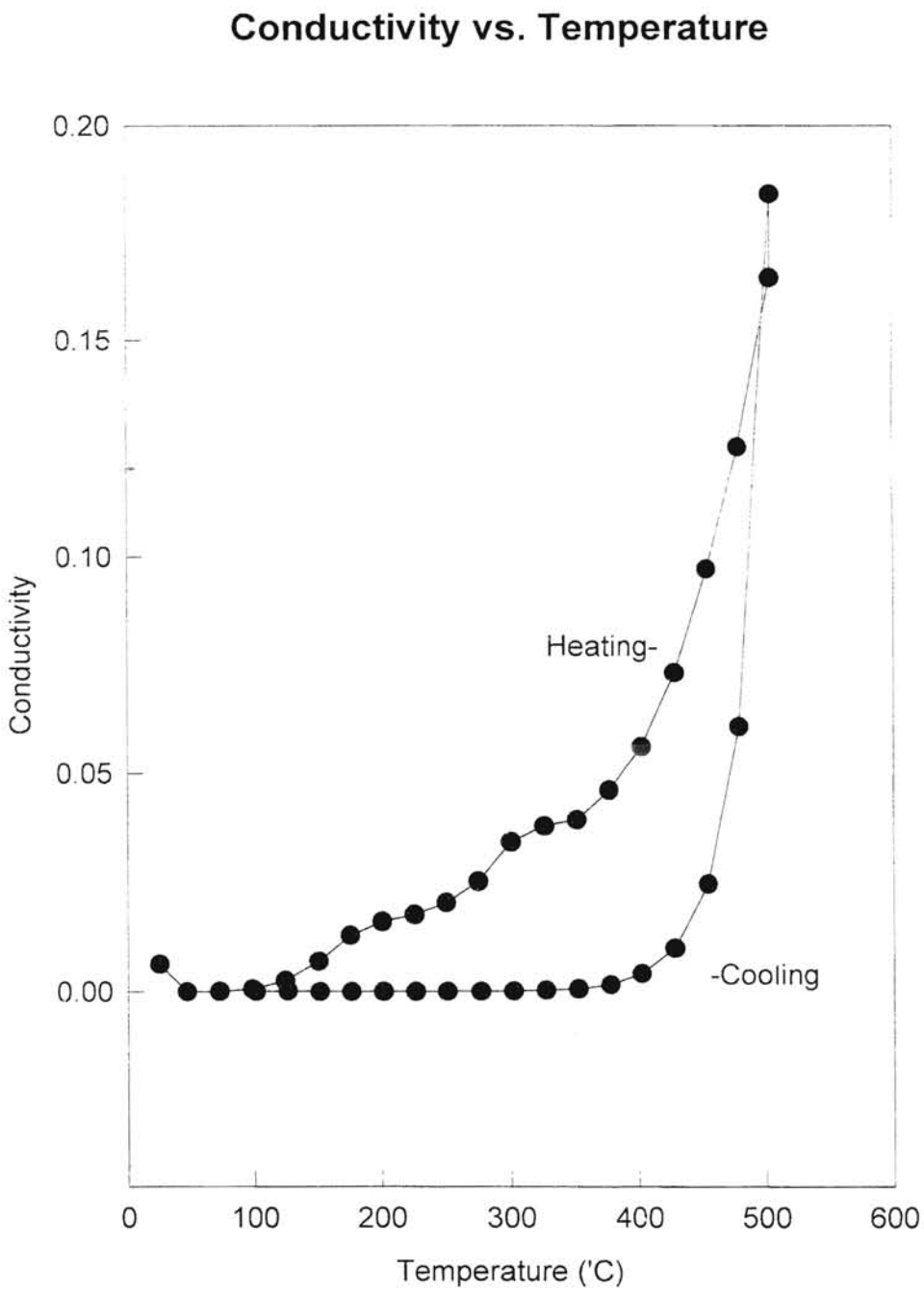

Figure 3.1: A typical graph of Conductivity vs. Temperature for a sample.

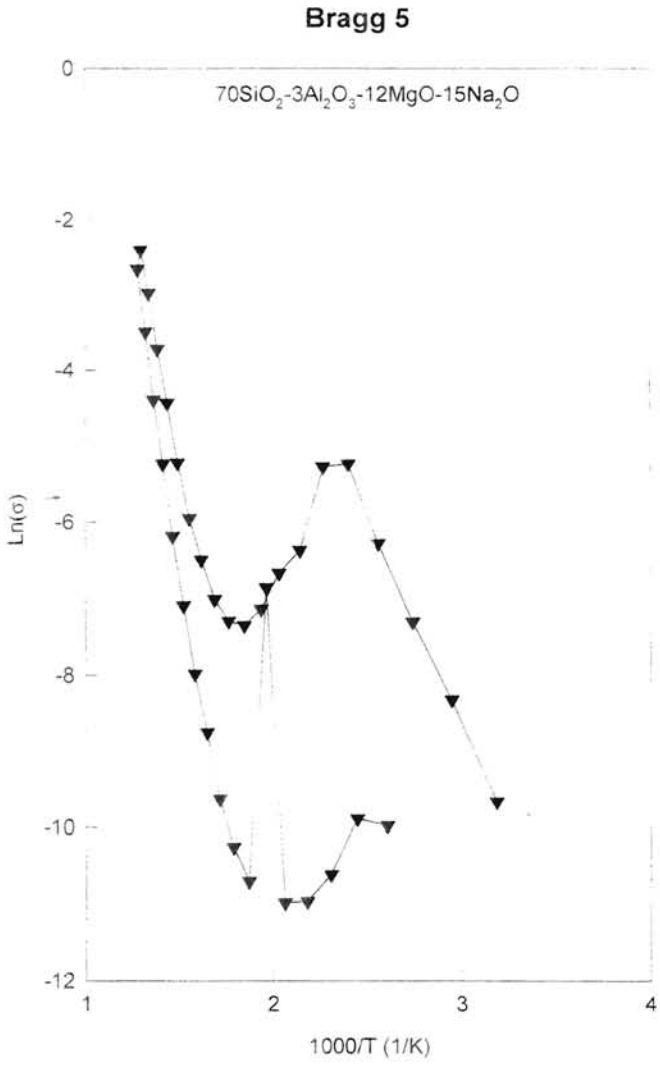

Figure 3.2: A typical graph of Ln(Conductivity) vs. 1000/Temperature for Bragg 5 whose molar composition is $70SiO_2$-$2Al_2O_3$-$12MgO$-$15Na_2O$.

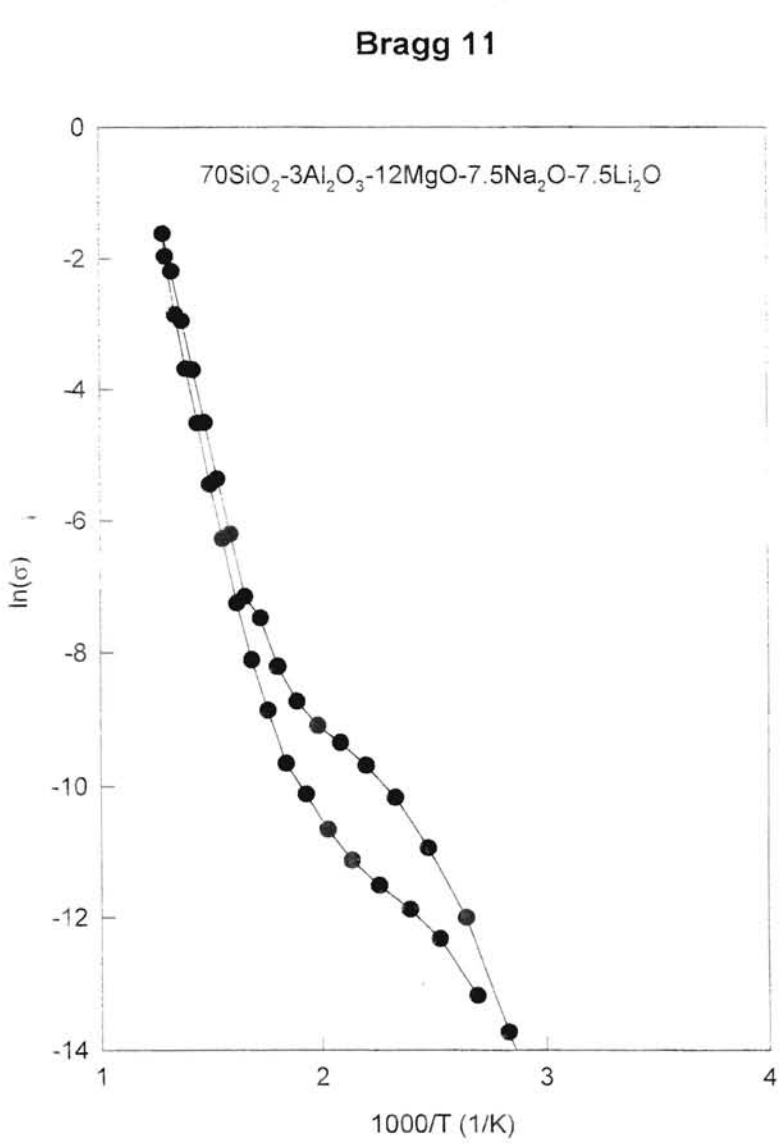

Figure 3.3: A typical graph of Ln(σ) vs. 1000/T for Bragg 11, whose molar composition is $70SiO_2$-$3Al_2O_3$-$12MgO$-$7.5Na_2O$-$7.5Li_2O$.

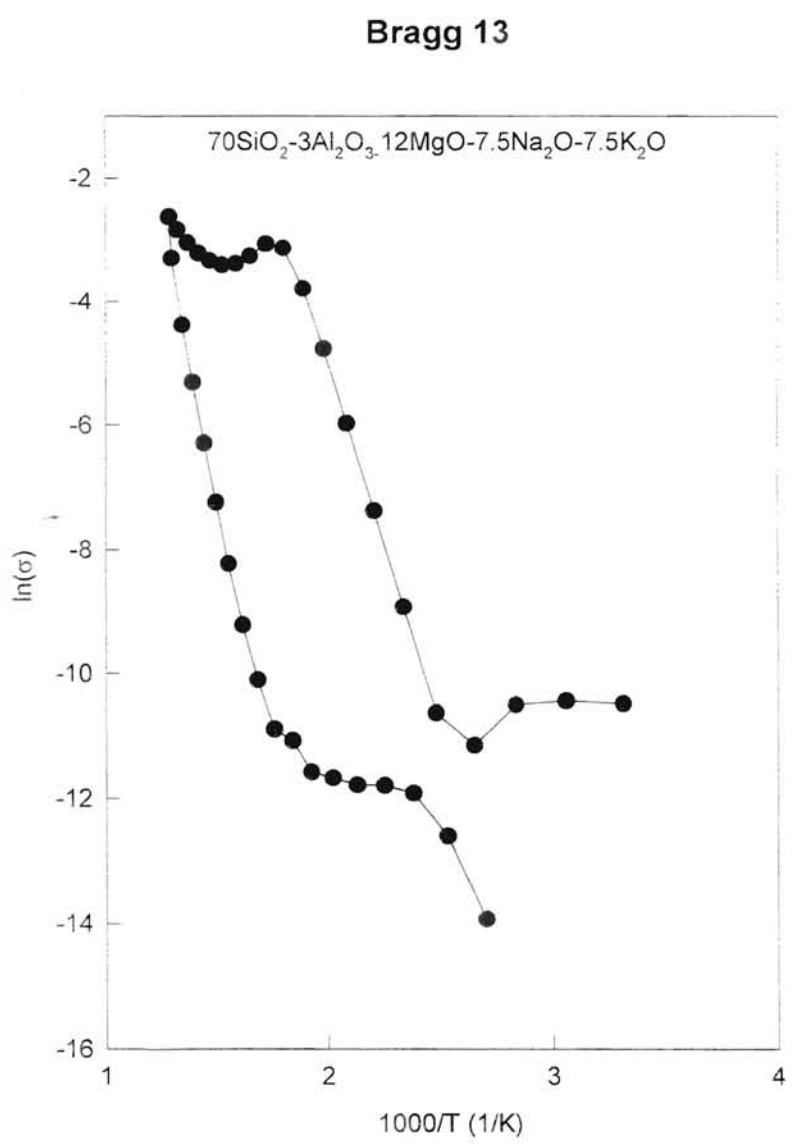

Figure 3.4: A typical graph of Ln(σ) vs. 1000/T for Bragg 13, whose molar composition is $70SiO_2$-$3Al_2O_3$-$12MgO$-$7.5Na_2O$-$7.5K_2O$.

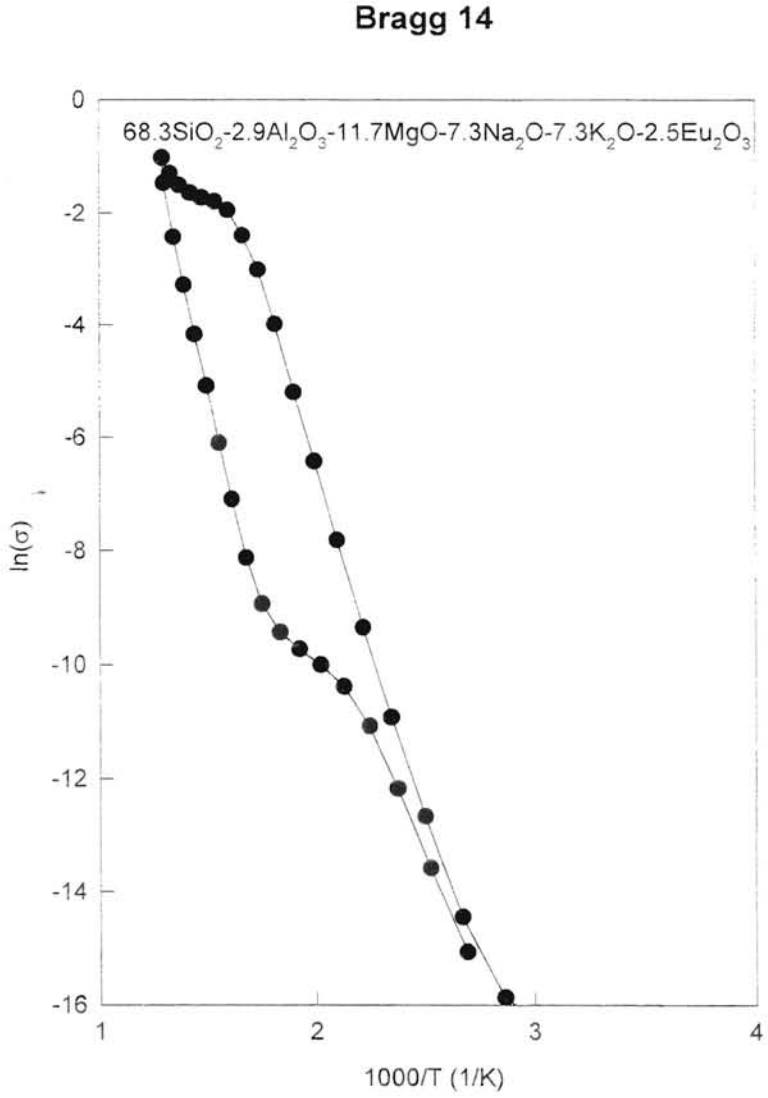

Figure 3.5: A typical graph of Ln(σ) vs. 1000/T for Bragg 14, whose molar composition is $68.3SiO_2$-$2.9Al_2O_3$-$11.7MgO$-$7.3Na_2O$-$7.3K_2O$-$2.5Eu_2O_3$.

would imply that the conductivity would be larger. Since potassium is larger that the other ions, this would seem like a plausible explanation. With the addition of a heavy earth metal, europium, with potassium to the glass; the conductivity also increased from the conductivity of the basic composition.

With the calculations of the conductivity complete, the activation energies can be tackled. The first step is to examine the correct equation. The Arrhenius equation discussed in Chapter 2 is appropriate.

$$\sigma = \sigma_0 \exp(E_a / k_b T)$$

As recalled from discussion in Chapter 2, if graphs are created with ln(σT) vs. 1000/T the activation energies follow quickly. By simple manipulation the slope of said graphs would be

$$\text{slope}=E_a/1000k_b$$

Where E_a is the observed activation energy and k_b is Boltzman's constant. Therefore the observed activation energy is equivalent to:

$$E_a=1000k_b(\text{slope})$$

Figure 3.6 through Figure 3.21 are the required graphs for each sample and respective run. The slope was calculated for several areas of each graph. With these slopes, the observed activation energies were found. Table IV through Table VII list the activation energies calculated for each sample. All of the energies were closely tied to the conductivity.

TABLE III

CONDUCTIVITY

	Largest Value ($1/\Omega cm$)	Initial ($1/\Omega cm$)
Bragg 5		
1st Run	1.842×10^{-1}	1.89×10^{-6}
2nd Run	1.055×10^{-1}	9.30×10^{-5}
3rd Run	2.795×10^{-1}	6.90×10^{-6}
4th Run	1.011×10^{-1}	4.64×10^{-5}
Bragg 11		
1st Run	3.118×10^{-1}	1.12×10^{-3}
2nd Run	1.577×10^{-1}	9.29×10^{-6}
3rd Run	4.941×10^{-1}	8.76×10^{-6}
4th Run	2.194×10^{-1}	4.33×10^{-6}
Bragg 13		
1st Run	7.527×10^{-2}	2.60×10^{-5}
2nd Run	5.944×10^{-3}	1.03×10^{-6}
3rd Run	6.107×10^{-3}	3.37×10^{-6}
4th Run	1.389×10^{-1}	5.05×10^{-7}
5th Run	1.634×10^{-1}	5.46×10^{-6}
Bragg 14		
1st Run	3.844×10^{-1}	6.22×10^{-8}
2nd Run	2.060×10^{-1}	5.22×10^{-6}
3rd Run	4.511×10^{-1}	2.87×10^{-5}

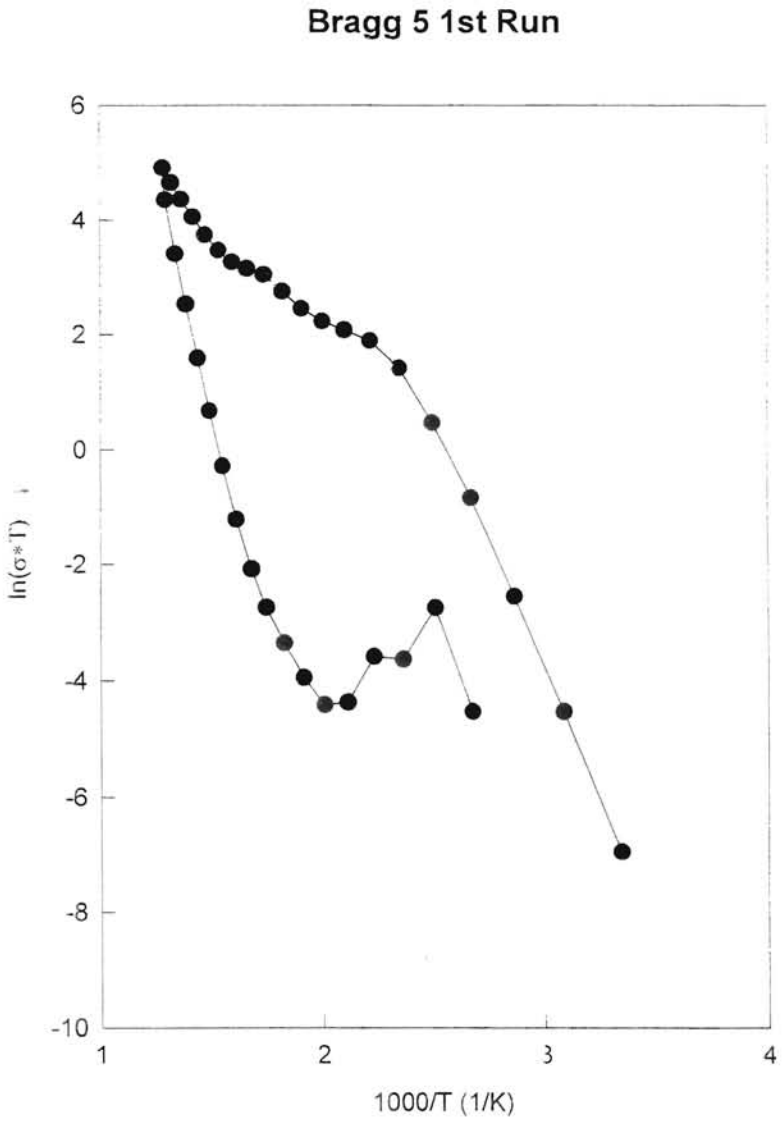

Figure 3.6: Graph of Ln(σ*T) vs. 1000/T for the first run of Bragg 5. The molar composition of Bragg 5 is $70SiO_2$-$2Al_2O_3$-12MgO-$15Na_2O$.

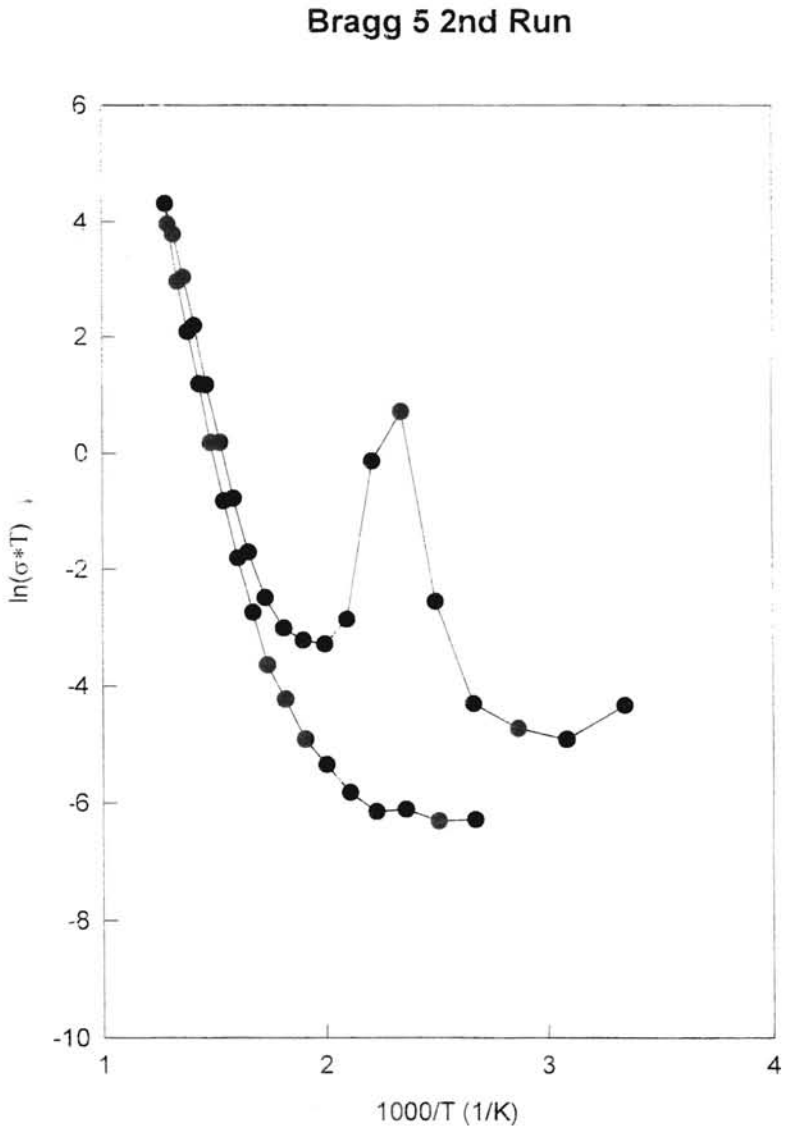

Figure 3.7: Graph of Ln(σ*T) vs. 1000/T for the second run of Bragg 5. The molar composition of Bragg 5 is $70SiO_2$-$2Al_2O_3$-12MgO-$15Na_2O$.

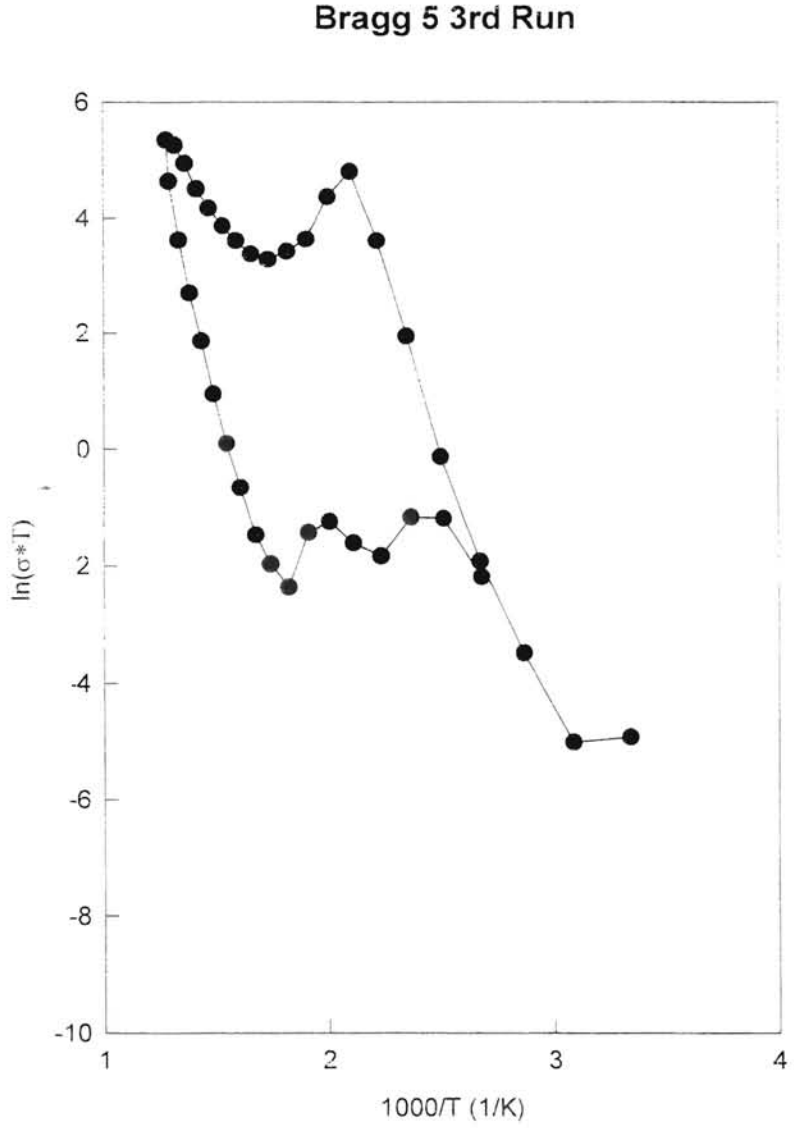

Figure 3.8: Graph of Ln(σ*T) vs. 1000/T for the third run of Bragg 5. The molar composition of Bragg 5 is $70SiO_2$-$2Al_2O_3$-12MgO-$15Na_2O$.

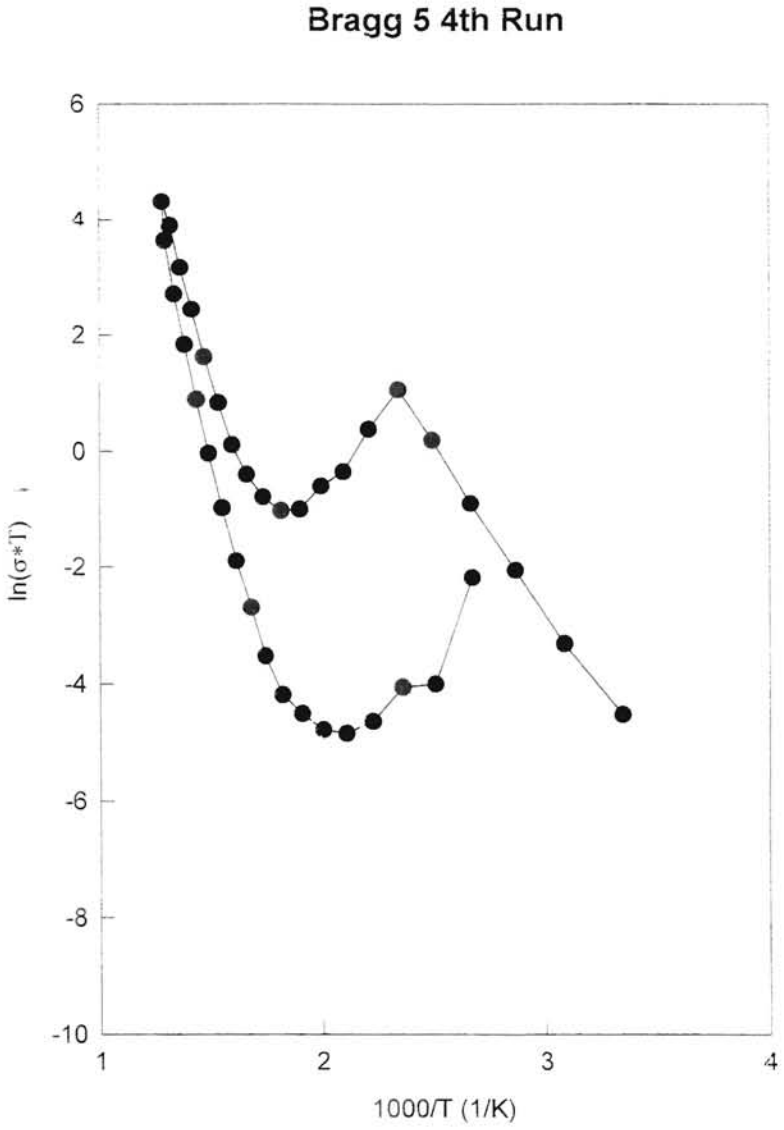

Figure 3.9: Graph of Ln(σ*T) vs. 1000/T for the fourth run of Bragg 5. The molar composition of Bragg 5 is $70SiO_2$-$2Al_2O_3$-12MgO-$15Na_2O$.

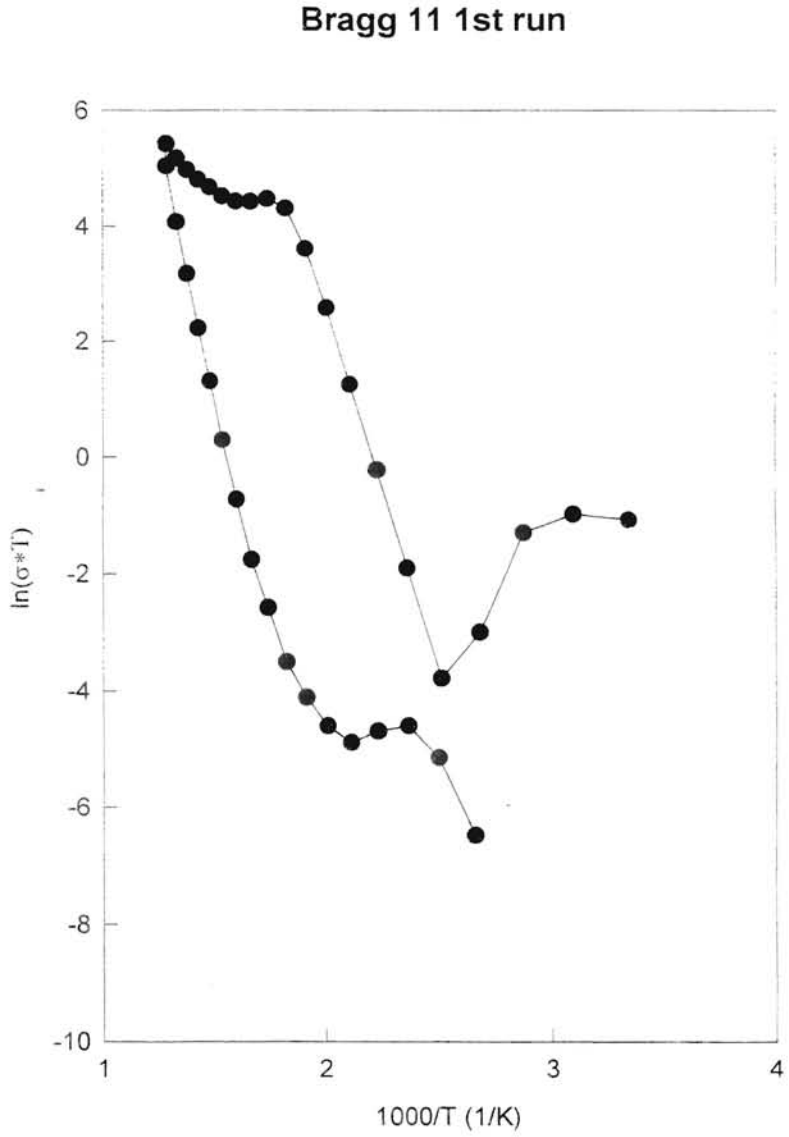

Figure 3.10: Graph of Ln(σ*T) vs. 1000/T for the first run of Bragg 11. The molar composition of Bragg 11 is $70SiO_2$-$3Al_2O_3$-12MgO-$7.5Na_2O$-$7.5K_2O$.

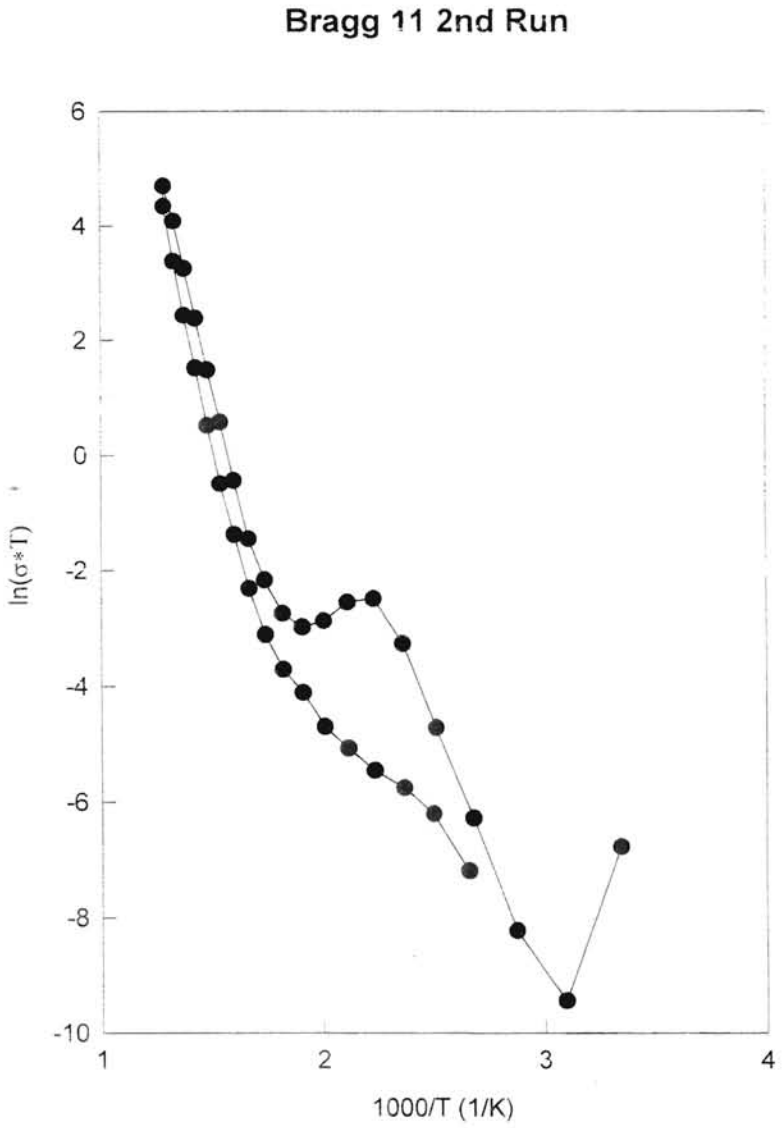

Figure 3.11: Graph of Ln(σ*T) vs. 1000/T for the second run of Bragg 11. The molar composition of Bragg 11 is $70SiO_2$-$3Al_2O_3$-12MgO-7.5Na_2O-7.5Li_2O.

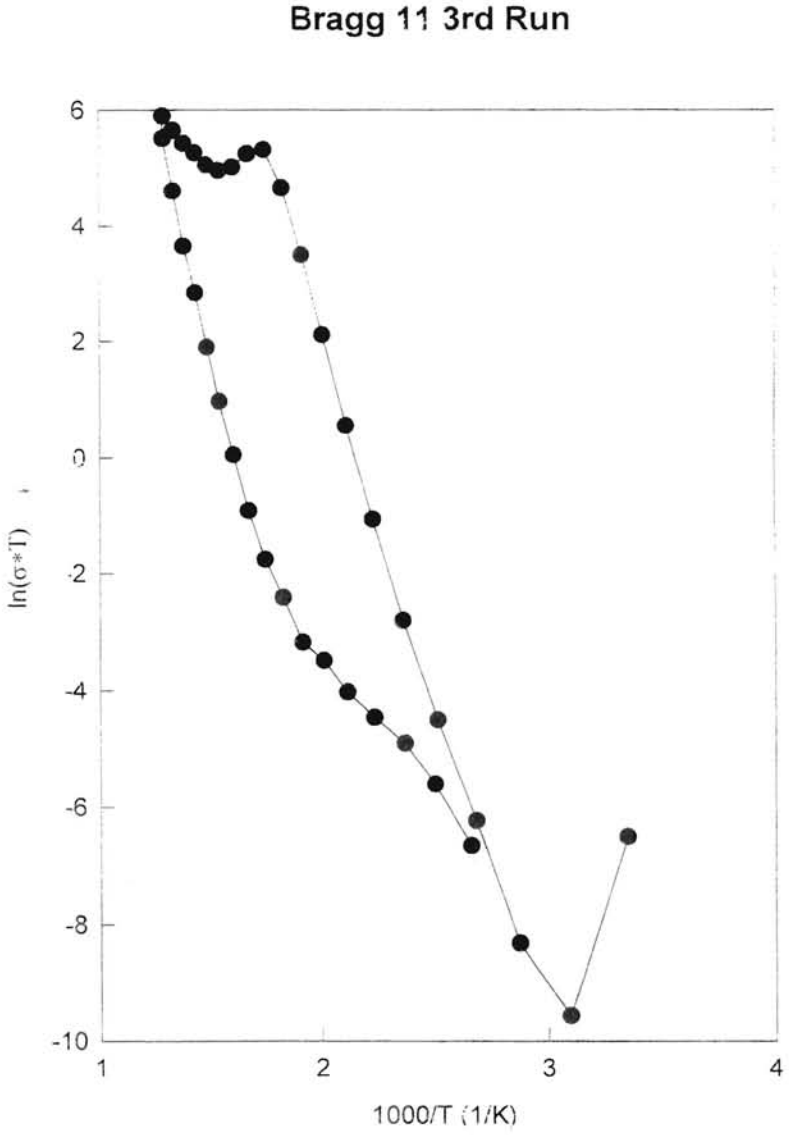

Figure 3.12: Graph of Ln(σ*T) vs. 1000/T for the third run of Bragg 11. The molar composition of Bragg 11 is $70SiO_2$-$3Al_2O_3$-12MgO-$7.5Na_2O$-$7.5Li_2O$.

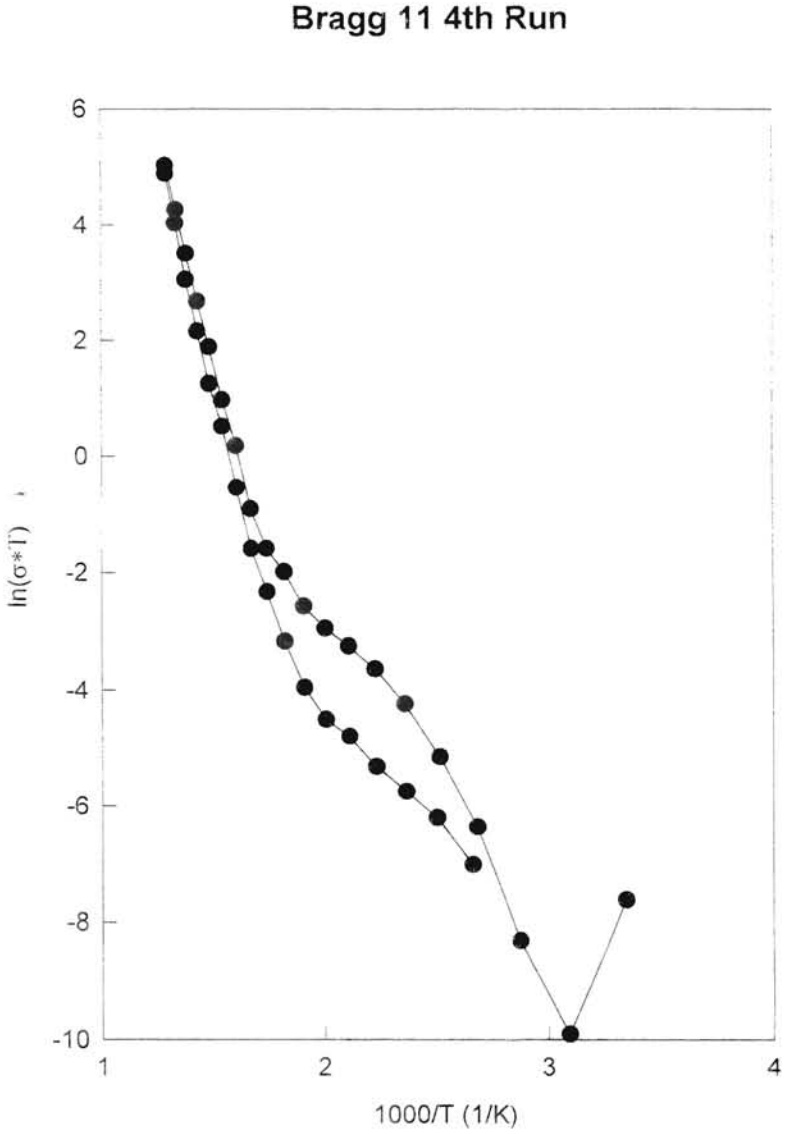

Figure 3.13: Graph of Ln(σ*T) vs. 1000/T for the fourth run of Bragg 11. The molar composition of Bragg 11 is $70SiO_2$-$3Al_2O_3$-12MgO-$7.5Na_2O$-$7.5Li_2O$.

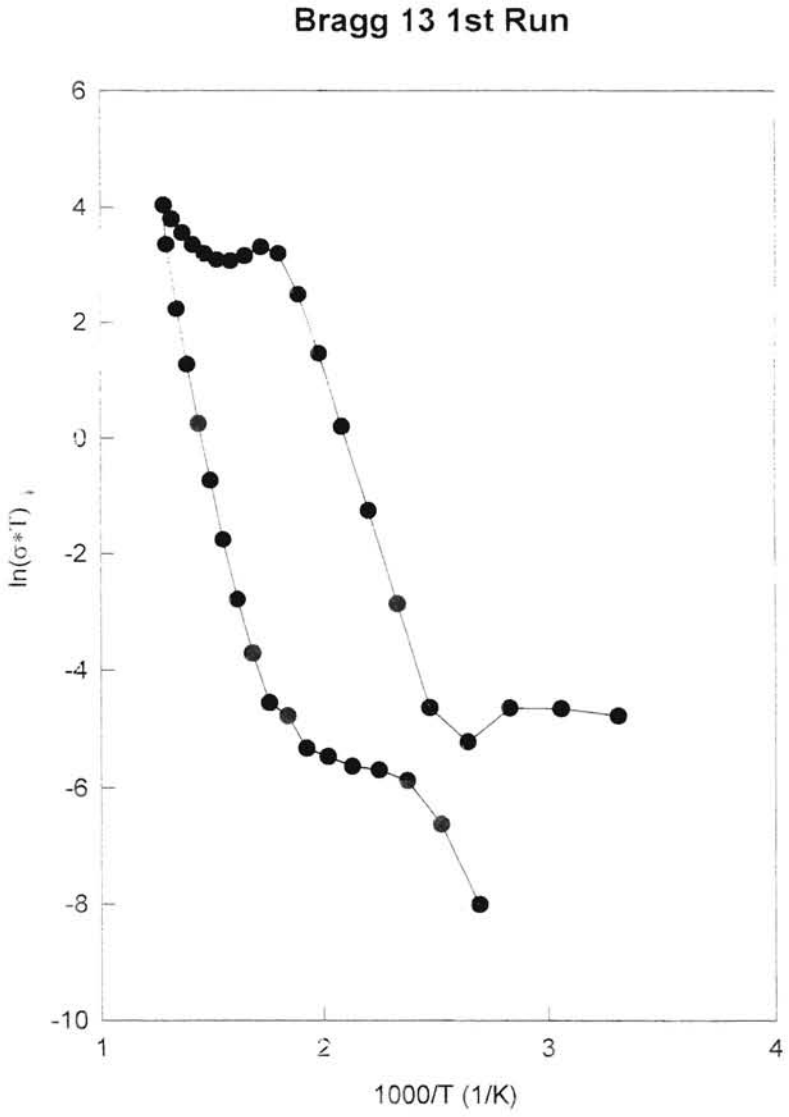

Figure 3.14: Graph of Ln(σ*T) vs. 1000/T for the first run of Bragg 13. The molar composition of Bragg 13 is $70SiO_2$-$3Al_2O_3$-12MgO-$7.5Na_2O$-$7.5K_2O$.

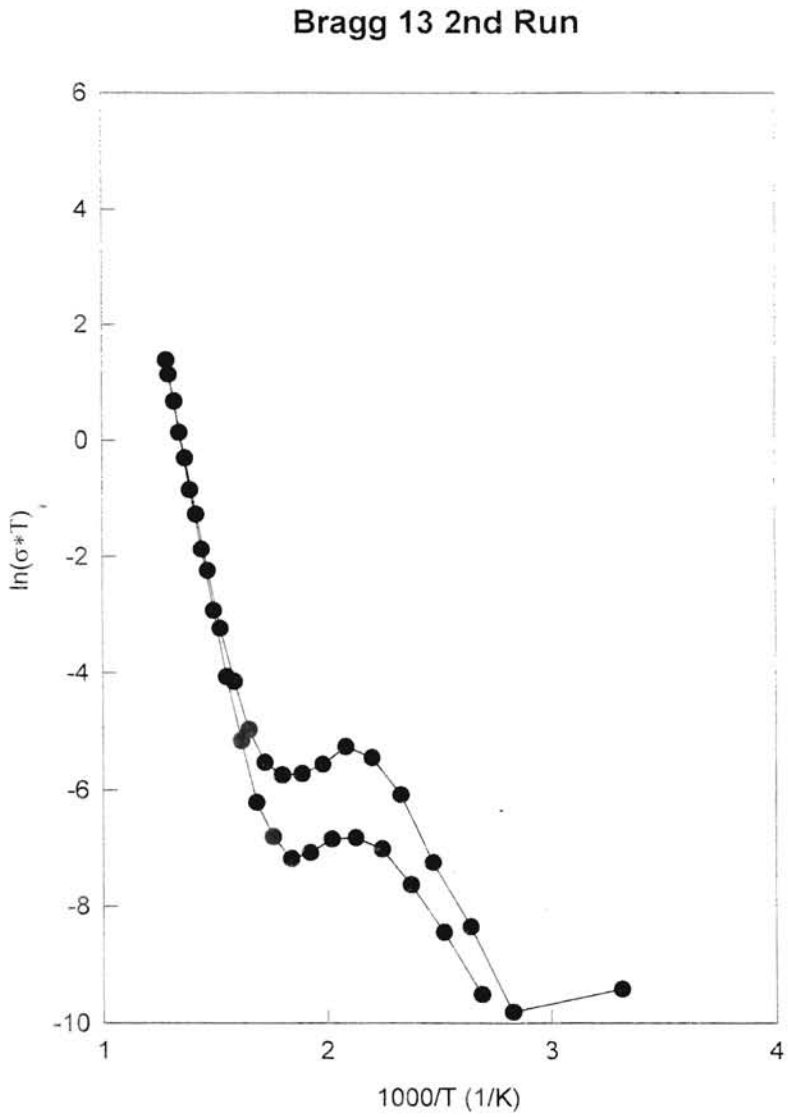

Figure 3.15: Graph of Ln(σ*T) vs. 1000/T for the second run of Bragg 13. The molar composition of Bragg 13 is $70SiO_2$-$3Al_2O_3$-12MgO-$7.5Na_2O$-$7.5K_2O$.

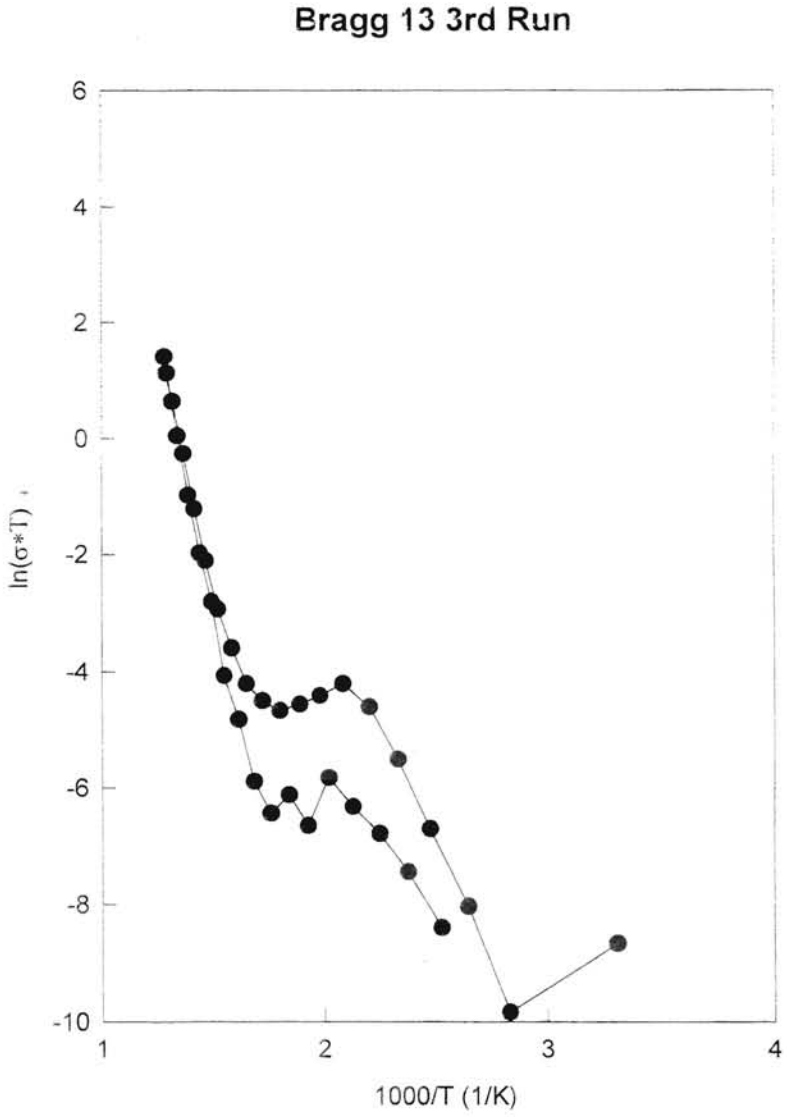

Figure 3.16: Graph of Ln(σ*T) vs. 1000/T for the third run of Bragg 13. The molar composition of Bragg 13 is $70SiO_2$-$3Al_2O_3$-12MgO-$7.5Na_2O$-$7.5K_2O$.

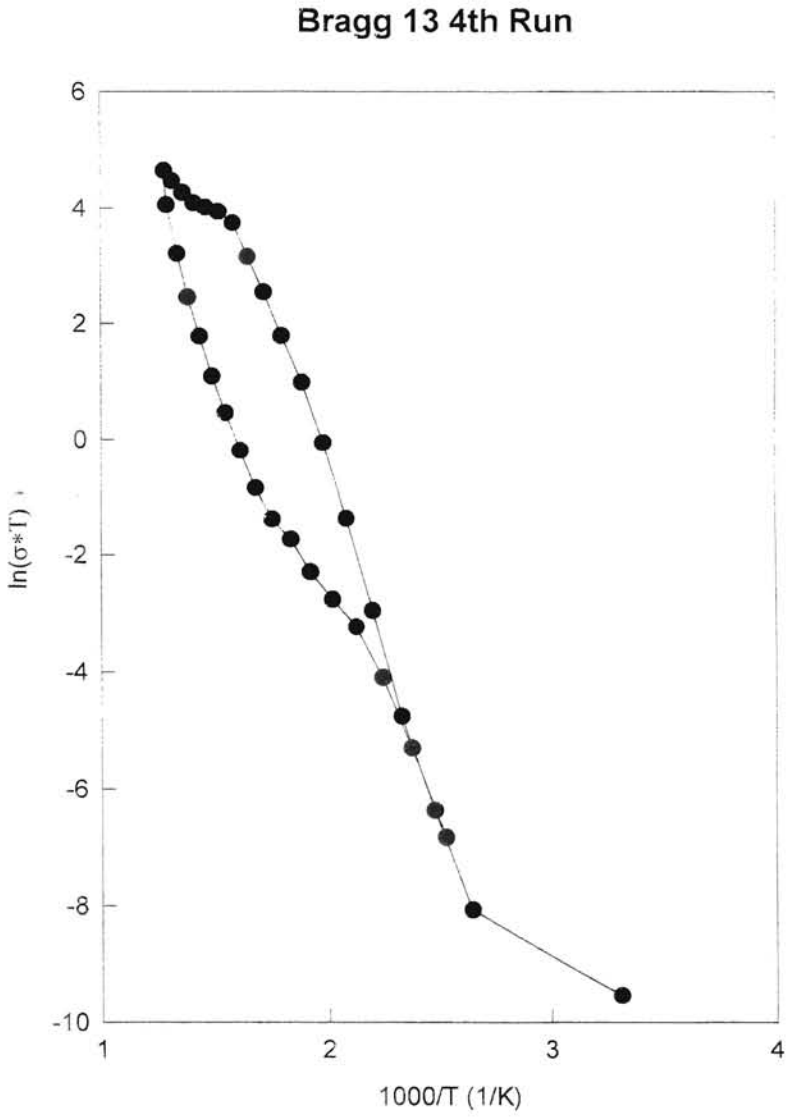

Figure 3.17: Graph of Ln(σ*T) vs. 1000/T for the fourth run of Bragg 13. The molar composition of Bragg 13 is $70SiO_2$-$3Al_2O_3$-12MgO-$7.5Na_2O$-$7.5K_2O$.

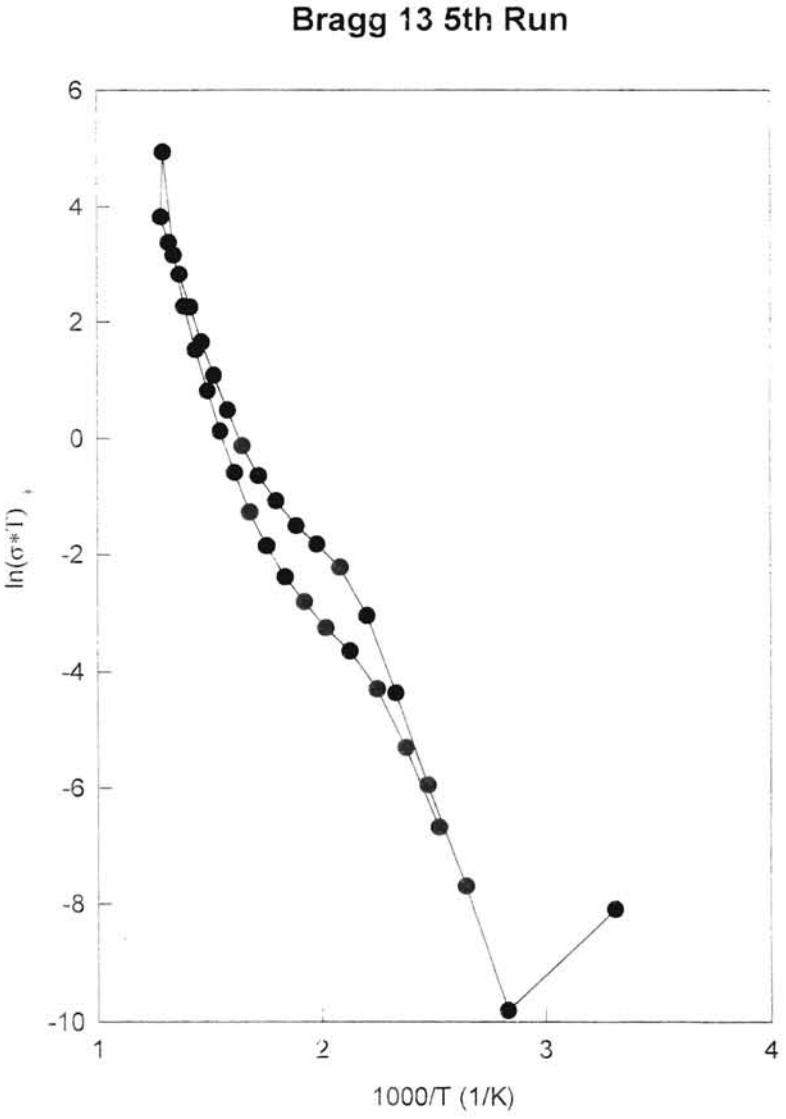

Figure 3.18: Graph of Ln(σ*T) vs. 1000/T for the fifth run of Bragg 13. The molar composition of Bragg 13 is $70SiO_2$-$3Al_2O_3$-12MgO-$7.5Na_2O$-$7.5K_2O$.

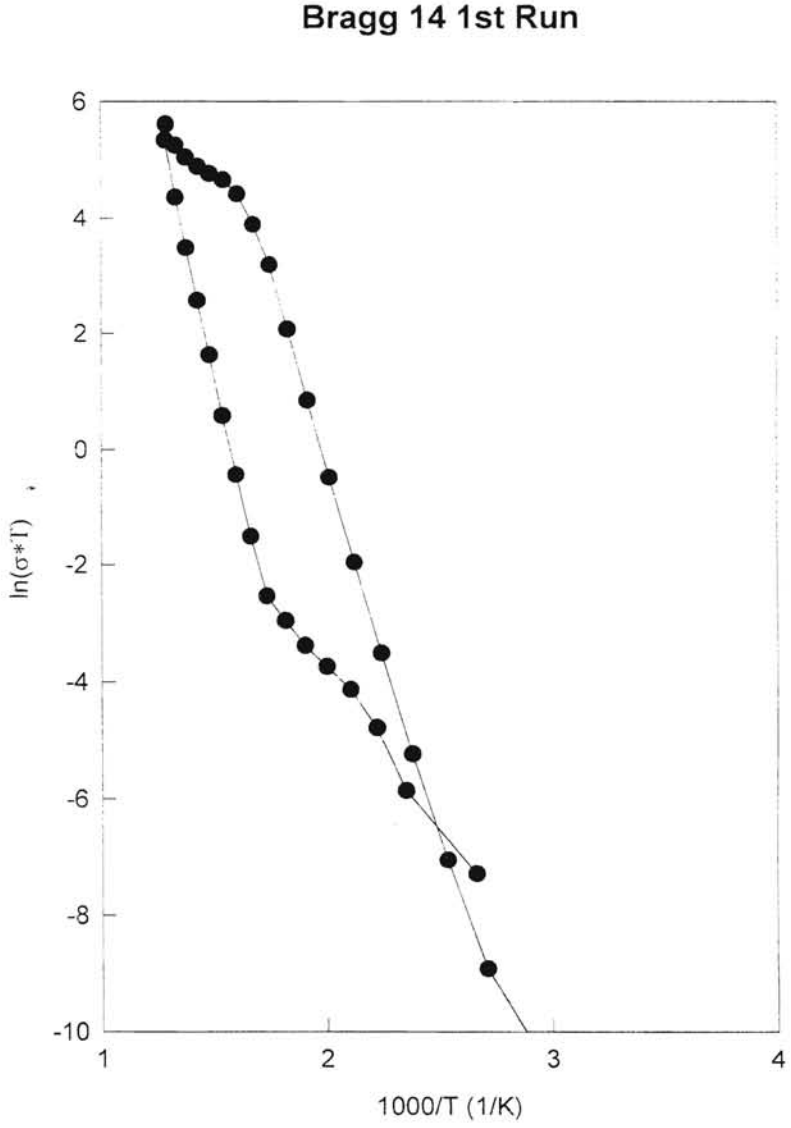

Figure 3.19: Graph of Ln(σ*T) vs. 1000/T for the first run of Bragg 14. The molar composition of Bragg 14 is $68.3SiO_2$-$2.9Al_2O_3$-11.7MgO-$7.3Na_2O$-$7.3K_2O$-$2.5Eu_2O_3$.

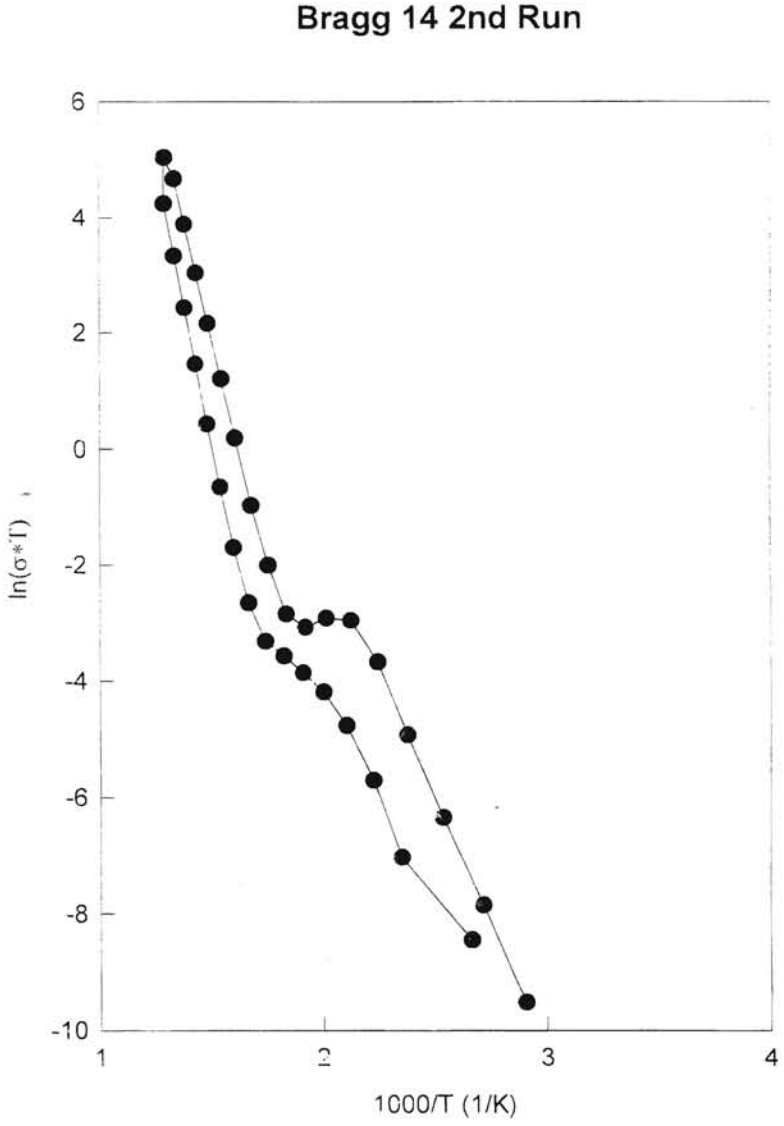

Figure 3.20: Graph of Ln(σ*T) vs. 1000/T for the second run of Bragg 14. The molar composition of Bragg 14 is 68.3SiO_2-2.9Al_2O_3-11.7MgO-7.3Na_2O-7.3K_2O-2.5Eu_2O_3.

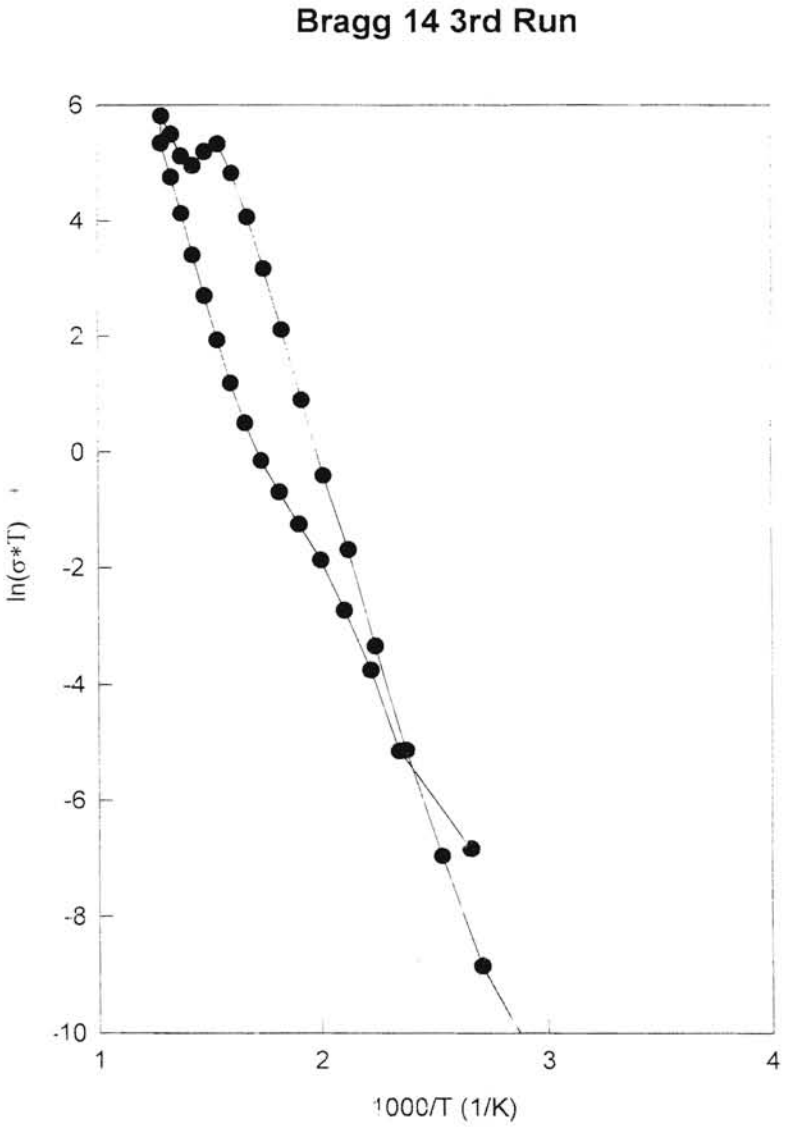

Figure 3.21: Graph of Ln(σ*T) vs. 1000/T for the third run of Bragg 14. The molar composition of Bragg 14 is $68.3SiO_2$-$2.9Al_2O_3$-$11.7MgO$-$7.3Na_2O$-$7.3K_2O$-$2.5Eu_2O_3$.

TABLE IV

ACTIVATION ENERGIES OF BRAGG 5

Run	Energy (eV)	Temperature Range (K)
1st	0.370	574-775
	1.335	775-548
2nd	1.340	574-775
	1.453	775-573
3rd	1.043	323-474
	0.483	599-749
	1.229	775-548
4th	0.486	599-775
	1.128	299-424
	1.350	775-548

TABLE V

ACTIVATION ENERGIES FOR BRAGG 11

Run	Energy (eV)	Temperature Range (K)
1st	1.062	398-524
	1.569	775-623
2nd	1.421	599-775
	1.574	775-623
3rd	1.210	424-549
	1.396	750-598
4th	1.285	575-755
	1.399	598-750

TABLE VI

ACTIVATION ENERGIES FOR BRAGG 13

Run	Energy (eV)	Temperature Range (K)
1st	1.042	399-525
	1.551	726-624
2nd	1.444	601-752
	1.753	778-650
3rd	1.567	626-778
	1.739	778-650
4th	1.106	399-626
	1.081	726-574
5th	0.944	348-449
	0.942	551-702
	0.819	726-547
	1.099	475-376

TABLE VII

ACTIVATION ENERGIES FOR BRAGG 14

Run	Energy (eV)	Temperature Range (K)
1st	1.097	446-623
	1.490	725-525
2nd	1.334	597-774
	1.427	700-550
3rd	1.101	395-648
	1.044	675-525

CHAPTER 4

CONCLUSION

A series of glasses, of similar yet different composition, were examined in this thesis. These glasses were Bragg 5, Bragg 11, Bragg 13, and Bragg 14. The composition of Bragg 5 was $70SiO_2$-$3Al_2O_2$-$12MgO$-$15Na_2O$ (molar percentages). Bragg 11 was $70SiO_2$-$3Al_2O_2$-$12MgO$-$7.5Na_2O$-$7.5Li_2O$ and Bragg 13's composition is $70SiO_2$-$3Al_2O_2$-$12MgO$-$7.5Na_2O$-$7.5K_2O$. Finally the composition of Bragg 14 is similar to that of Bragg 13 except with the addition of europium, $68.3SiO_2$-$2.9Al_2O_2$-$11.7MgO$-$7.5Na_2O$-$7.3K_2O$-$2.5Eu_2O_3$. It is apparent that the differences in these compositions are due to the addition of various alkalis.

These samples were subjected to a constant voltage with an increasing temperature. The data collected was then used to examine the conductivity of the samples. It was noted that although the mixed alkali effect was not seen, the changes in conductivity were easily explained. With the addition of the smaller of the ions, the conductivity increase. This implies that it was more convenient for the smaller ions to move throughout the network. When the larger, potassium, ions were added the conductivity therefore decrease which is in agreement with the earlier discussion. When an rare earth metal, europium, was added the conductivity increased. This increase was expected from this large ion expanding the network.

The calculation of the activation energies will be used to analyze the temperature dependence of four wave mixing of these samples. This has yet to be done. The activation energies for the samples corresponded with the conductivity. Bragg 13, which experienced the smallest conductivity, registered the largest activation energies. The more freely the ions move throughout the network, the smaller the energies they must overcome. This direct correlation indicates that the increase in the population of mobile ions is the major contributor to the temperature dependence of the conductivity in the temperature range studied here.

REFERENCES

1. Griscom, David L. Defect Structure of Glasses: Some Outstanding Questions in Regard to Vitreous Silica. N. J. Kreitl Honorary Symposium, Vienna, July 2-5, 1984.

2. Maass, Pilipp, Bunde, Armin, and Ingram, Malcolm D. "Ion Transport Anomalies in Glasses." Physical Review Letters, Vol. 68(20), 3064-3067.

3. Angell, C. A. "Mobile Ions in Amorphous Solids." Annual Review of Physical Chemistry, Vol. 43, 693-717.

4. Kamitsos, E. I., Patsis, A. P., Chrssikos, G. D., and Kapoutsis, J. A. "Structural Aspects of the Mixed Alkali Effect." Chimik Chronika, New Series, Vol. 23(2-3), 245-250 (1994).

5. Angell, C. A. "Correlation of Mechanical and Electrical Relaxation Phenomena in Superionic Conducting Glasses." Materials Chemistry and Physics, Vol. 23, 143-169.

6. Ingram, M. D., Maass, P., and Bunde, A. "Ion Mobility and Structural Relaxation in Glasses." Chimica Chronica, New Series, Vol. 23, 221-226 (1994).

7. Kittel, Charles. Introduction to Solid State Physics, John Wiley & Sons, New York 1986.

8. Ingram, Malcolm D. Materials Science And Technology: A comprehensive Treatment, (R. W. Cahn, P. Haasen, E. J. Kramer, Ed.), Vol. 9, 718-750.

9. Angell, C. A. "Dynamic Processes in Ionic Glasses." Chemical Review, Vol. 90, 523-542, 1990.

VITA

Lynett Rock

Candidate for the Degree of

Master of Science

Thesis: IONIC CONDUCTIVITY IN BRAGG GLASSES.

Major Field: Physics

Biographical:

Personal Data: Born in Claremore, Oklahoma on October 21, 1972, the daughter of Calvin and Joyce Rock.

Education: Graduated from Warner High School, Warner, Oklahoma in May, 1990; received Bachelor of Science degree in Engineering Physics from Northeastern State University, Tahlequah, Oklahoma in May, 1994. Completed the requirements for the Master of Science degree with a major in Physics at Oklahoma State University in July, 1996.

Experience: Employed as an undergraduate lab assistant; Northeastern State University, Department of Physics, 1993-1994. Employed as a graduate teaching assistant and research assistant; Oklahoma State University, 1994-present.

Professional Memberships: American Indian Science and Engineering Society.